International Journal of Science and Research (IJSR)
ISSN (Online): 2319-7064
Index Copernicus Value (2013): 6.14 | Impact Factor (2013): 4.438

Artificial Neural Network Controller for Induction Motor Drive

Aakanksha Tripathi[1], Naveen Asati[2]

[1]M.Tech-Scholar (Control Systems), Department of Electrical and Electronics Engineering, LNCT, Bhopal (M.P), India
[2]Department of Electrical and Electronics Engineering, LNCT, Bhopal (M.P), India

Abstract: ***Induction motors are being applied today to a wider range of applications requiring variable speed. Generally, variable speed drives for Induction Motor require both wide operating range of speed and fast torque response, regardless of any disturbances and uncertainties (like load variation, parameters variation and un-modeled dynamics). This leads to more advanced ANN control methods to meet the real demand. The recent advances in the area of field-oriented control along with the rapid development and cost reduction of power electronics devices and microprocessors have made variable speed induction motor drives an economical alternative for many industrial applications. These AC drives are nowadays replacing their DC counterpart and are becoming a major component in today's sophisticated industrial manufacturing and process automation. Advent of high switching frequency PWM inverters has made it possible to apply sophisticated control strategies to AC motor drives operating from variable voltage, variable frequency source. In the formulation of any control problem there will typically be discrepancies between the actual plant and the mathematical model developed for controller design. This mismatch may be due to un-modeled dynamics, variation in system parameters or the approximation of complex plant behavior by a straightforward model. The designer must ensure that the resulting controller has the ability to produce required performance levels in practice despite such plant/model mismatches .In this dissertation report, a sliding mode controller is designed for an induction motor drive. The gain and band width of the controller is designed considering rotor resistance variation, model in accuracies and load disturbance, to have an ideal speed tracking. The chattering effect is also taken into account. The controller is simulated under various conditions and a comparative study of the results with that of ANN controller has been presented.***

Keywords: Induction motor drive, ANN controlled, SimuLink, MATLAB, Inverter

1. Introduction

Induction motors are the most important workhorses in industry and they are manufactured in large numbers. About half of the electrical energy generated in a developed country is ultimately consumed by electric motors, of which over 90 % are induction motors. For a relatively long period, induction motors have mainly been deployed in constant-speed motor drives for general purpose applications. The rapid development of power electronic devices and converter technologies in the past few decades, however, has made possible efficient speed control by varying the supply frequency, giving rise to various forms of adjustable-speed induction motor drives. In about the same period, there were also advances in control methods and artificial intelligence (AI) techniques, including expert system, fuzzy logic, neural networks and genetic algorithm. Researchers soon realized that the performance of induction motor drives can be enhanced by adopting artificial-intelligence-based methods.

Since the 1990s, AI-based induction motor drives have received greater attention. In recent years, scientists and researchers have acquired significant development on various sorts of control theories and methods. Among these control technologies, intelligent control methods, which are generally regarded as the aggregation of fuzzy logic control, neural network control, genetic algorithm, and expert system, have exhibited particular superiorities. Artificial Intelligent Controller (AIC) could be the best controller for Induction Motor control. Over the last two decades researchers have been working to apply AIC for induction motor drives [1-6]. This is because that AIC possesses advantages as compared to the conventional PI, PID and their adaptive versions. Mostly, it is often difficult to develop an accurate system mathematical model since the unknown and unavoidable parameter variations, and unknown load variation due to disturbances, saturation and variation temperature. High accuracy is not usually imperative for most of the induction motor drive, however high performance IM drive applications, a desirable control performance in both transient and steady states must be provided even when the parameters and load of the motor varying during the operation. Controllers with fixed parameters cannot provide these requirements unless unrealistically high gains are used. Thus, the conventional constant gain controller used in the variable speed induction motor drives become poor when the uncertainties of the drive such as load disturbance, mechanical parameter variations and unmodelled dynamics in practical applications. Therefore control strategy must be adaptive and robust. As a result several control strategies have been developed for induction motor drives with in last two decades. The Artificial Intelligence (AI) techniques, such as Expert System (ES), Fuzzy Logic (FL), Artificial Neural Network (ANN or NNW) and Genetic Algorithm (GA) have recently been applied widely in power electronics and motor drives. This paper presents the speed control scheme of vector controlled induction motor drive involves decoupling of the speed and ref speed into torque and flux producing components. Artificial Neural Network based control scheme is simulated. The performance of artificial neural network based controller's is compared with that of the conventional proportional integral controller.

2. Mathematical Model of the Induction Motor

During the entire report, a complex vector notation and some reference frame conversions are used. Since this is quite essential to the understanding of the rest of the theory.

Torque Production

If a IM's rotor is initially stationary, its conductor will be subjected to a sweeping magnetic field, produced by stator's current, inducing current in the short-circuit rotor with same frequency. The interaction of air gap flux and rotor mmf produces torque. At synchronous speed, the rotor cannot have any induced currents and; therefore, torque cannot be produced. At any other speed, there will be a difference between the rotating field (synchronous) speed and the shaft speed, which is called slip speed. The slip speed will induce current and torque in the rotor. The rotor will move in the same diction as that of the rotating magnetic field to reduce the induced current. We define slip as:

$$s = \frac{N_e - N_r}{N_e} = \frac{\omega_e - \omega_r}{\omega_e} = \frac{\omega_{sl}}{\omega_e}$$

Where ωe = stator supply frequency （r/s), ωr = rotor electrical speed（r/s), and ωsl = slip frequency（r/s). The rotor current is induced at slip frequency. Since the rotor is moving at speed ωr and it current wave is moving at speed ωsl relative to the rotor, the rotor mmf wave moves at the same speed as that of the air gap flux wave the torque expression can be derived as..

$$T_e = \pi(\frac{p}{2})lrB_pF_p \sin\delta$$

Where P = number of poles, l = axial length of the machine, r = machine radius, Bp = peak value of air gap flux density, Fp = peak value of rotor mmf, and δ is defined as the torque angle.

Equivalent Circuit

A simple steady state equivalent circuit model of an induction motor is a very important tool for analysis and performance prediction under steady-state conditions.

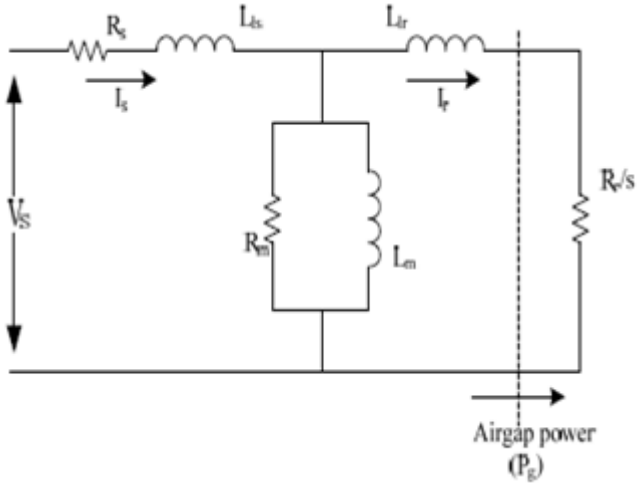

Figure 1: Steady state equivalent circuit of induction motor

Figure 3.5 shows the steady-state equivalent circuit (with core loss neglected) for the analysis and design of induction motor. In the equivalent circuit, all rotor parameters are referred to the stator. For the equivalent circuit of Figure (10), Rs is the stator resistance, Rr is the rotor resistance, Lm is the magnetizing inductance, L1s is the stator leakage inductance and L1r is the rotor leakage inductance and s is the slip. Two additional quantities, stator and rotor inductance, are now defined as:

$$L_s = L_{ls} + L_m \text{ And } L_r = L_{lr} + L_m$$

The various power expressions can be written form the equivalent circuit of Figure (10.) as follows:

$$T_e = \pi(\frac{p}{2})lrB_pF_p \sin\delta$$

Input Power:

Stator Copper loss: $P_{ls} = 3I_s^2R_s$

Core loss: $P_{lc} = \frac{3V_m^2}{R_m}$

Power across air gap: $P_g = 3I_r^2\frac{R_r}{S}$

Rotor copper loss: $P_{lr} = 3I_r^2R_r$

Output power: $P_o = P_g - P_{lr} = 3I_r^2R_r\frac{1-s}{s}$

Since the output power is the produce of developed torque Te and speed ωm, Te can be expressed as

$$T_e = \frac{P_o}{\omega_m} = \frac{3}{\omega_m}I_r^2R_r\frac{1-s}{s} = 3\left(\frac{P}{2}\right)I_r^2\frac{R_r}{S\omega_e}$$

The equivalent circuit of Figure 3.2 can be simplified to that shown in Figure 2.3, where the core loss resistor m R has been dropped and the magnetizing inductance Lm has been shifted to the input. This approximation is easily justified for an integral Horsepower machine, where

$$\left|(R_s + j\omega_eL_{ls})\right| << \omega_eL_m$$

The performance prediction by the simplified circuit typically varies within 5 percent from that of the actual machine. In Figure (10), the current Ir is figured out by:[15]

$$I_r = \frac{V_s}{\sqrt{\left(R_s + R_r/S\right)^2 + \omega_e^2\left(L_{ls} + L_{lr}\right)^2}}$$

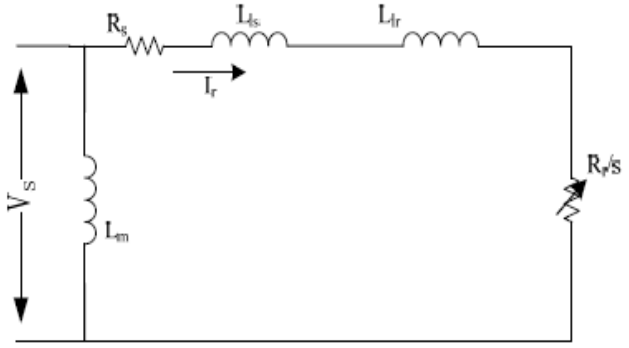

Figure 2: Approximate Per phase equivalent circuit of induction motor

$$T_e = 3\left(\frac{P}{2}\right)\frac{R_r}{S\omega_e}\frac{V_s^2}{\left(R_s + R_r/S\right)^2 + \omega_e^2\left(L_{ls}+L_{lr}\right)^2}$$

A further simplification of the equivalent circuit of Figure (11) can be made by neglecting the stator parameters Rs and Lls. This assumption is not unreasonable for an integral horsepower machine, particularly if the speed is typically above 10

$$T_e = 3\left(\frac{P}{2}\right)\left(\frac{V_s}{\omega_e}\right)^2\frac{\omega_{sl}R_r}{R_r^2+\omega_{sl}^2L_{lr}^2}$$

percent.

Where $\omega_{sl} = S\omega_e$ .The air gap flux can be given by

$$\psi_m = \frac{V_s}{\omega_e}$$

In a low-slip region, (12) can be approximated as

$$T_e = 3\left(\frac{P}{2}\right)\frac{1}{R_r}\left(\psi_m\right)^2\omega_{sl}$$

Where $R_r^2 >> \omega_{sl}^2L_{lr}^2$ Equation is critical for following analysis because it indicated that at constant flux, the torque is proportional to slip frequency, or at constant slip frequency, torque is proportional to flux.[15,21]

Three-Phase Transformations

In the study of generalized machine theory, mathematical transformations are often used to decouple variables, to facilitate the solutions of difficult equations with time varying coefficients, or to refer all variables to a common reference frame.

The most commonly used transformation is the polyphase to orthogonal two-phase (or two-axis) transformation. For the n-phase to two-phase case, it can be expressed in the form:

$$\left[f_{xy}\right] = \left[T(\theta)\right]\left[f_{1,2,.....n}\right]$$

Where,

$$\left[T(\theta)\right] = \sqrt{\frac{2}{3}}\begin{bmatrix}\cos\frac{p}{2}\theta\cos\left(\frac{p}{2}\theta-\alpha\right).....\cos\left(\frac{p}{n}\theta-(n-1)\alpha\right)\\ \sin\frac{p}{2}\theta\sin\left(\frac{p}{2}\theta-\alpha\right).....\sin\left(\frac{p}{n}\theta-(n-1)\alpha\right)\end{bmatrix}$$

And the electrical angle between the two adjacent magnetic axes of a uniformly distributed n-phase windings. The coefficient $\sqrt{2/n}$, is introduced to make the transformation power invariant.

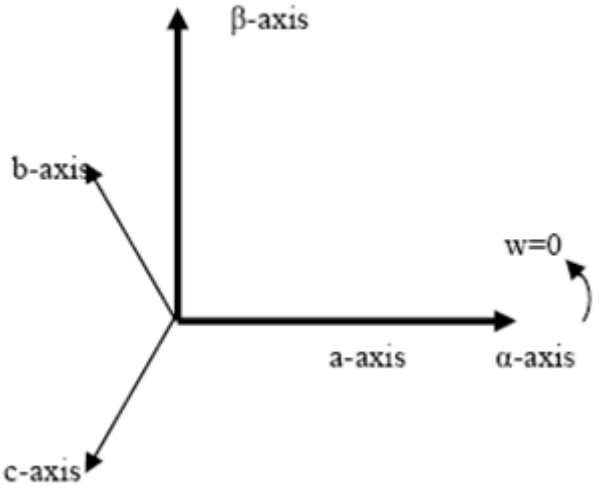

Figure 3: Relationship between the $\alpha\beta$ abc quantities

Clark Transformations

The Clark transformation is basically employed to transform three-phase to two-phase quantities. The two-phase variables in stationary reference frame are sometimes denoted as α and β . As shown in Fig(.14) the α axis coincides with the phase-a axis and the β axis lags the α axis by 90^0 .

$$\left[f_{\alpha\beta0}\right] = \left[T_{\alpha\beta0}\right]\left[f_{abc}\right]$$

Where the transformation matrix, $[T\alpha\beta0]$ is given by:

$$\left[T_{\alpha\beta0}\right] = \frac{2}{3}\begin{pmatrix}1 & -\frac{1}{2} & -\frac{1}{2}\\ 0 & \sqrt{\frac{3}{2}} & -\sqrt{\frac{3}{2}}\\ \frac{1}{2} & \frac{1}{2} & \frac{1}{2}\end{pmatrix}$$

The inverse transformation is:

$$\left[T_{\alpha\beta 0}\right]^{-1} = \frac{2}{3}\begin{pmatrix} 1 & 0 & 1 \\ -\frac{1}{2} & \sqrt{\frac{3}{2}} & 1 \\ -\frac{1}{2} & -\sqrt{\frac{3}{2}} & 1 \end{pmatrix}$$

Park Transformations

The Park's transformation is a well-known transformation that converts the quantities to to-phase synchronously rotating frame. The transformation is in the form of:

$$\left[f_{dq0}\right] = \left[T_{dq0}(\theta_d)\right]\left[f_{abc}\right]$$

Where the dq0 transformation matrix is defined as:

$$\left[T_{dq0}(\theta_d)\right] = \frac{2}{3}\begin{pmatrix} \cos\theta_d & \cos\left(\theta_d - \frac{2\pi}{3}\right) & \mathrm{COS}\left(\theta_d + \frac{2\pi}{3}\right) \\ -\sin\theta_d & -\sin\left(\theta_d - \frac{2\pi}{3}\right) & -\sin\left(\theta_d + \frac{2\pi}{3}\right) \\ \frac{1}{2} & \frac{1}{2} & \frac{1}{2} \end{pmatrix}$$

And the inverse is given by;

$$\left[T_{dq0}(\theta_d)\right]^{-1} = \begin{pmatrix} \cos\theta_d & -\sin\theta_d & 1 \\ \cos\left(\theta_d - \frac{2\pi}{3}\right) & -\sin\left(\theta_d - \frac{2\pi}{3}\right) & 1 \\ \mathrm{COS}\left(\theta_d + \frac{2\pi}{3}\right) & -\sin\left(\theta_d + \frac{2\pi}{3}\right) & 1 \end{pmatrix}$$

Where θ_d is transformation angle, the relationship between them θ_d and θ_q is:

$$\theta_q = \theta_d + \frac{\pi}{2}$$

One can show that $\left[T_{dq0}\right]$ and $\left[T_{qd0}\right]$, are basically the same, except for the ordering of the d and q variables. Both of the alternatives are shown figure

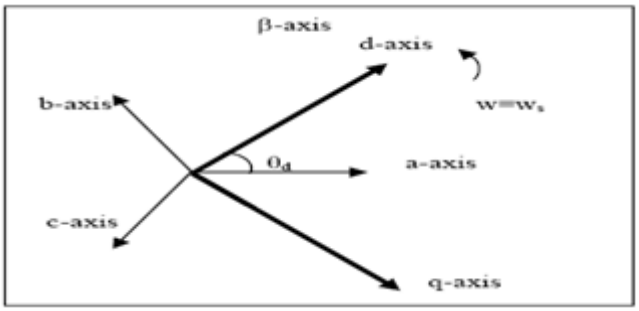

Figure 4: Relationship between the dq and the abc quantities

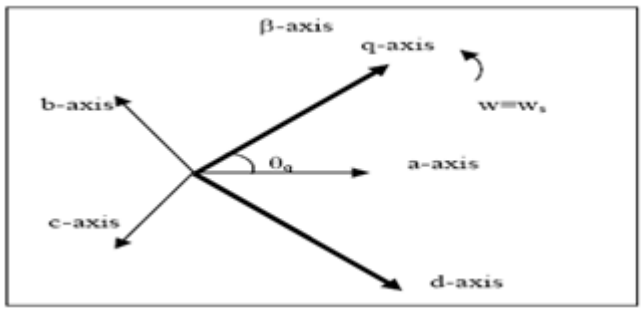

Figure 5: Relationship between the qd and the abc quantities

Where Lls is the per phase stator winding leakage inductance, Llr is the per phase rotor winding leakage inductance, Lss is the self inductance of the stator winding, Lrr is the self inductance of the rotor winding, Lsm is the mutual inductance between stator windings, Lrm is the mutual inductance between rotor windings, and Lsr is the peak value of the stator to rotor mutual inductance. Note that the idealized machine is described by six first-order differential equations, one for each winding. These differential equations are coupled to one another through the mutual inductance between the windings. In particular, the statot-rotor coupling terms vary with time. Transformations like the dq or can facilitate the computation of the transient solution of the above induction motor model by transforming the differential equations with time-varying inductances to differential equations with constant inductances.-axis is as follows:

3. Inverters

Three phase inverters, supplying voltages and currents of adjustable frequency and magnitude to the stator, are an important element of adjustable speed drive systems employing induction motors. Inverters with semiconductor power switches are d.c. to a.c. static power converters. Depending on the type of d.c. source supplying the inverter, they can be classified as voltage source inverters (VSI) or current source inverters (CSI). In practice, the d.c. source is usually a rectifier, typically of the three phase bridge configuration, with d.c. link connected between the rectifier and the inverter. The d.c. link is a simple inductive, capacitive, or inductive-capacitive low-pass filter. Since neither the voltage across a capacitor nor the current through an inductor can change instantaneously. A capacitive-output d.c. link is used for a VSI and an inductive-output link is employed in CSI.VSIs can be either voltage or current controlled. In a voltage-controlled inverter, it is the frequency and magnitude of the fundamental of the output voltage that is adjusted. Feed-forward voltage control is employed, since the inverter voltage is dependent only on the supply voltage and the states of the inverter switches, and, therefore, accurately predictable. Current controlled VSIs require sensors of the output currents which provide the necessary control feedback. The type of semiconductor power switch used in an inverter depends on the volt-ampere rating of the inverter, as well as on other operating and economic considerations, such as switching frequency or cost of the system.[23] Taking into account the transient- and steady-state requirements, we have used 1200V, 40A IGBT switches. With appropriate heat sink, we can rise to 20 KHz, however a10KHz, switching losses and conduction losses

become equal, moreover, complex mathematical algorithms require much time. Thus 10 KHz is selected as the switching frequency in our algorithms.

A diagram of the power circuit of a three phase VSI is shown in the Fig.2.14. The circuit has bridge topology with three branches (phases), each consisting of two power switches and two freewheeling diodes. In the case illustrated and implemented in this thesis, the inverter is supplied from an uncontrolled, diode-based rectifier, via d.c. link which contains an LC filter in the inverted configuration. While this circuit represents a standard arrangement, it allows only positive power flow from the supply system to the load via typically three-phase power line. Negative power flow, which occurs when the load feeds the recovered power back to the supply, is not possible since the resulting negative d.c. component of the current in the d.c. link cannot pass through the rectifier diodes. Therefore, in drive systems where the VSI-fed motor may not operate as a generator, more complex supply system must be used. These involve either a braking resistance connected across the d.c. link or replacement of the uncontrolled rectifier by a dual converter. As a future work, the inverter may be supported with braking resistance connected across the d.c. link via freewheeling diode and a transistor. When the power is returned by the motor, it is dissipated in the braking resistor which is called dynamic braking.[24] The circuit diagram of three-phase VSI used in this project is shown in Fig.3.14n

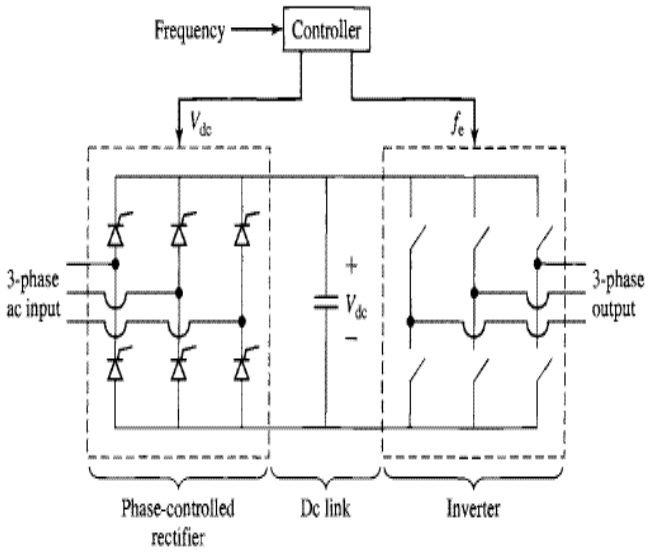

Figure 6: Circuit diagram of three phase voltage source inverter

Because of the constraints that the input lines must never be shorted and the output current must always be continuous, a voltage source inverter can assume only eight distinct operational topologies.

4. Neural Network

A Neural Network (NN) is an information-processing system that has some performance characteristics in common with biological neural networks. A Neural Network consists of a set of highly interconnected simple nonlinear processing elements called neurons, units, cells or nodes. Each neuron is connected to the other neurons by means of direct communication links where each has an associated weight. The weight represents information being used by the network to solve the problem.

A neural network can achieve desired input-output mapping with a specified set of weights stored in the connections between neurons, and can be trained to do a particular job by adjusting the weights on each connection.

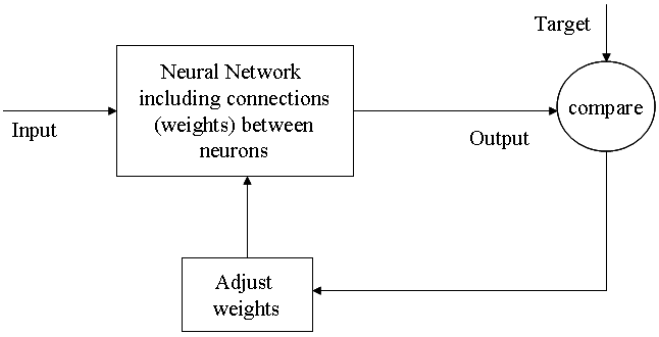

Figure 7: shows a situation where the network is adjusted, based on a comparison of the output and the target, until the network output matches the target [4].

Typically many such input/target pairs are needed to train a network. The adjust weights block in the Fig.3.1 adjusts the weights according to the error obtained from output and target.

5. Simple Neuron Model

Each neuron has an internal state, called its activation or activity level, which is a function of inputs it has received. Typically a neuron sends its activation as a signal to several other neurons.

Fig. illustrates a simple neuron model in which x_1, x_2 and x_3 are the inputs and w_1, w_2 and w_3 are corresponding weights respectively. The net input, y_1 is the sum of the weighted inputs from x_1, x_2, and x_3 and bias i.e.

$$y_1 = w_1x_1+w_2x_2+w_3x_3+b$$

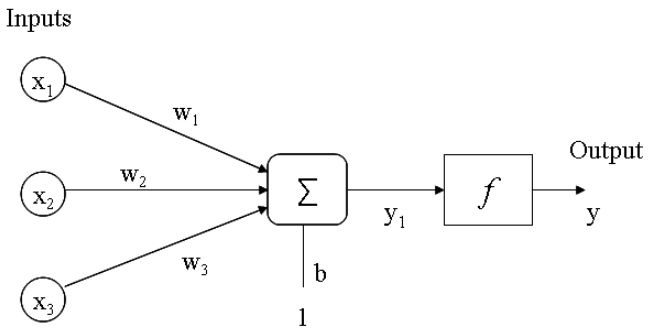

Figure 8: Simple Neuron Model

The net-input, y_1 is passed to the activation function f to get the output y.

6. Proposed Model

Majority of induction motor drives are of open-loop, constant-v/f, voltage-source-inverter fed type. These drives are cost effective but they offer sluggish response. Due to

high current transients during the torque changes, they are subject to undesirable trips. To avoid the unnecessary trips, the control parameters like acceleration/deceleration rate have to be adjusted (reduced) according to the load. This results in under-utilization of torque capability of the motor. Thus, the drawback of v/f drive can be attributed to lack of torque control. This is the reason why open-loop, constant-v/f drives are mostly used in low performance fan and pump type loads. In this paper, we propose a modified control scheme that includes the torque control and a current regulated PWM inverter to avoid the undesirable trips due to transient currents. The feedback signals, that is, torque and rotor speed are obtained from the dc link quantities. For the accuracy of these estimated quantities, the reconstructed ac line current waveforms should be correct. The accuracy of reconstructed waveforms depends upon the sampling rate. Higher the sampling rate less is the error between the actual and reconstructed waveforms. In a hard-switching inverter, the switching frequency is limited to a typical value of a few kHz. This limits the sampling rate of dc current and hence the update rate of torque and rotor speed using dc link quantities only. Consequently, closing the loop directly on the instantaneous value of the estimated torque now becomes difficult because estimation error during a PWM cycle could become significantly high. In fact, instantaneous error at the sampling instant could have a different polarity from the average error over one PWM cycle. In order to use the estimated torque in a more robust manner, a control strategy should use the averaged torque instead of the instantaneous value. In this system, ANN controllers are used to regulate the average value of torque and speed respectively. The output of the ANN controller regulators forms the q-axis command current in a synchronously rotating reference frame.

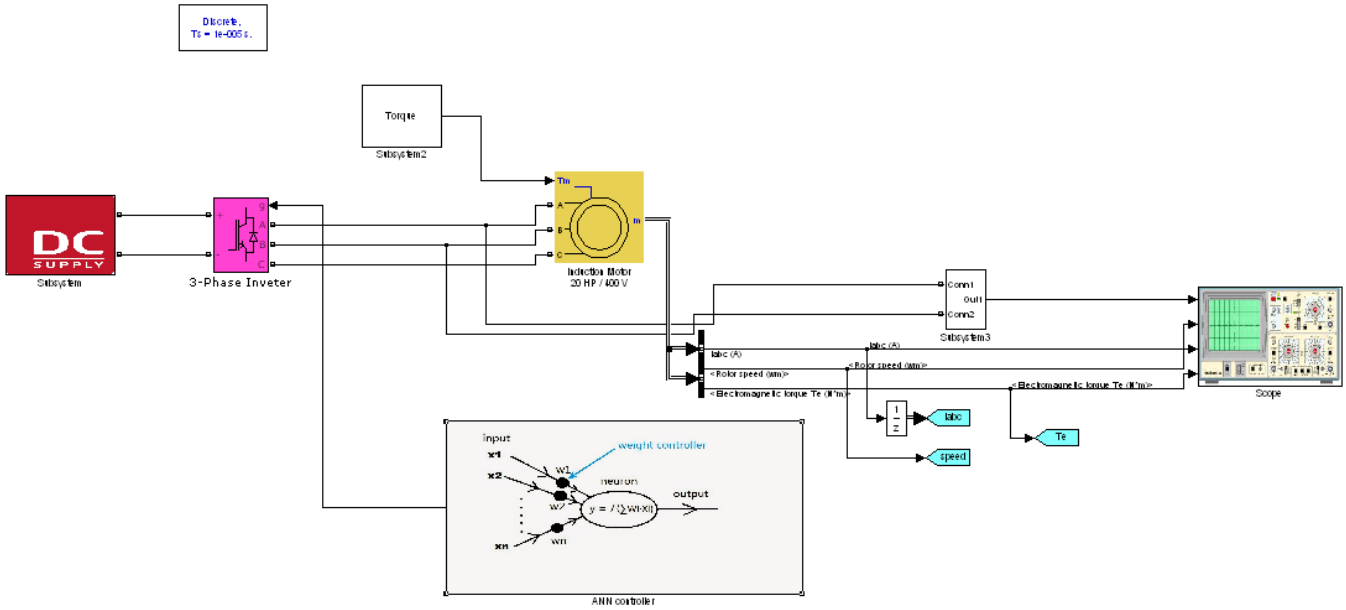

7. Results

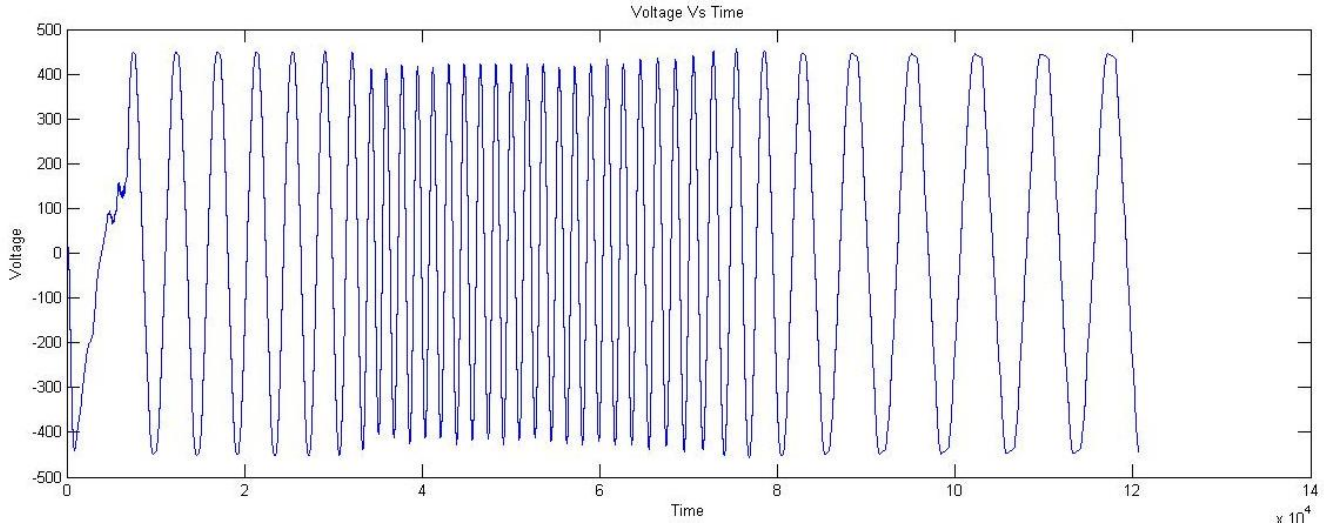

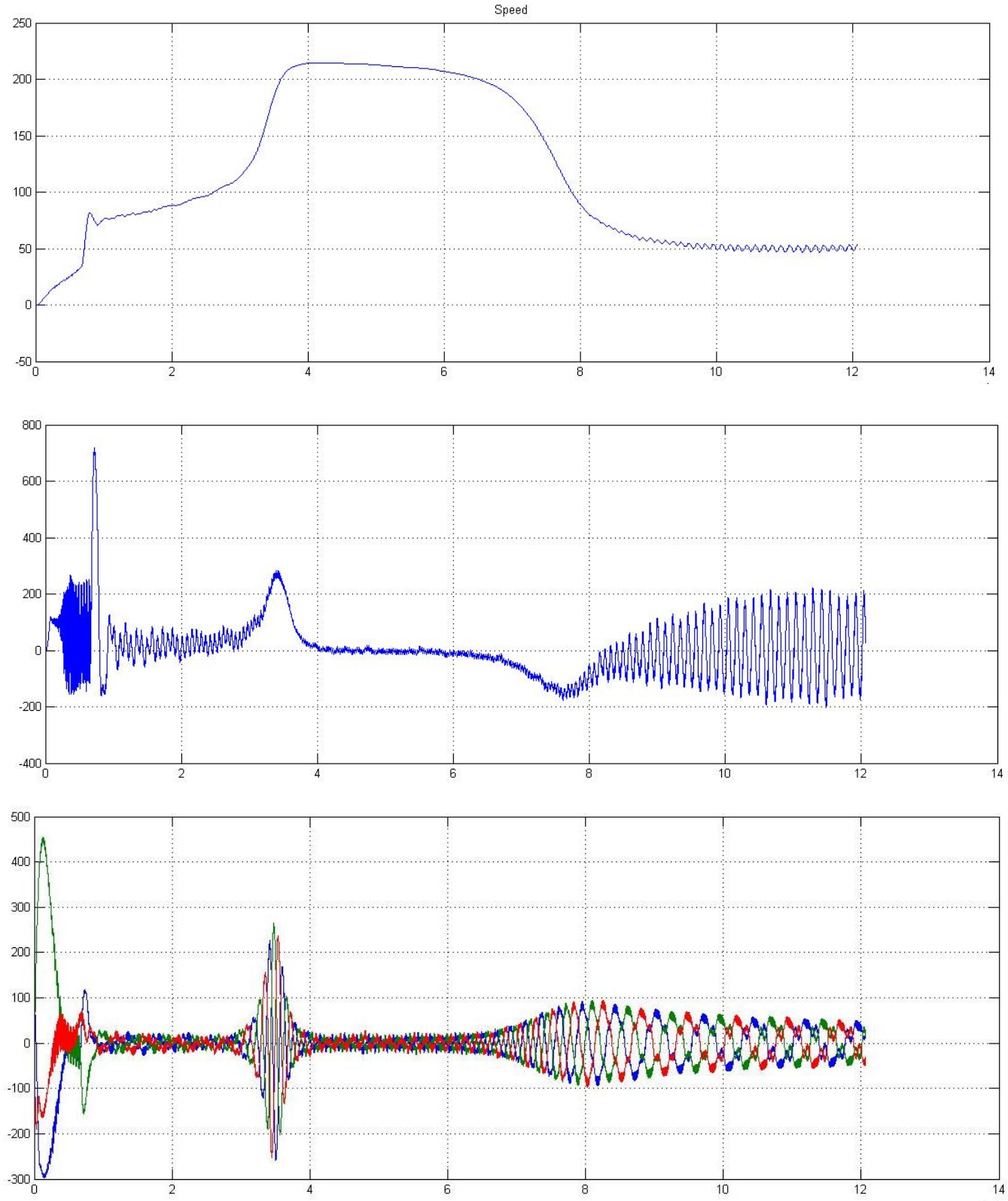

8. Conclusion

In this paper the theory of ANN controller is studied in detail. The equations of the induction motor model are reorganized so as to apply the control technique. The ANN controller gain and band width are designed, considering various factors such as rotor resistance variation, model in accuracies, load torque disturbance and also to have an ideal speed tracking. Considering the case such as load disturbance, the response of the designed sliding mode controller is satisfactory. It also gives good trajectory tracking performance. The speed regulation characteristic is also satisfactory. We discuss the results with ANN controller.

References

[1] Bor-Ren Lin "Power converter control based on neural and fuzzy methods" Power Electronics Research Laboratory, Elsevier 2014.

[2] G. Durgasukumar, M.K. Pathak "Comparison of adaptive Neuro-Fuzzy-based space-vector modulation for two-level inverter" 2014
[3] Fábio Limaa, Walter Kaiserb, Ivan Nunes da Silvac, Azauri A.A. de "Open-loop neuro-fuzzy speed estimator applied to vector and scalar induction motor drive" 2014 Elsevier .
[4] Yuksel Oguz, Mehmet Dede "Speed estimation of vector controlled squirrel cage asynchronous motor with artificial neural networks"2014
[5] Czeslaw T. Kowalski, Teresa Orlowska-Kowalska "Neural networks application for induction motor faults diagnosis"
[6] Bogdan Pryymak, Juan M. Moreno-Eguilaz, Juan Peracaula 1 "Neural network flux optimization using a model of losses in Induction motor drives" 18 April 2006
[7] Tsai-Jiun Ren, Tien-Chi Chen" Robust speed-controlled induction motor drive based on recurrent neural network". (2006)
[8] Tiago Henrique dos Santosa, Alessandro Goedtelb, Sergio Augusto Oliveira da Silvab, Marcelo Suetakec "Scalar control of an induction motor using a neural sensor less technique."
[9] J.M. Gutierrez-Villalobos a,n, J.Rodriguez-Resendiz a, E.A.Rivas-Araiza a, V.H.Mucino b "A review of parameter estimators and controllers for induction motors
[10] Raj M. Bharadwaja,1, Alexander G. Parlosb, Hamid A. Toliyata "Neural speed filtering for sensor less induction motor drives" May 2002;
[11] Abdalla, Zulkeflee Khalidin, motor Based on Neural network Inverse Control.
[12] Maiti S, Chakraborty C, Hori Y, Ta Minh. C (2008). Model reference adaptive controller-based rotor resistance and speed estimation techniques for FOC led induction motor drive utilizing reactive power, IEEE. Trans. Ind. Electron 55(2): 594-601.
[13] Lascu C, Boldea I, Blaabjerg F (2004). Direct torque control of sensorless induction motor drives: A sliding mode approach, IEEE Trans. Ind. Appl. 40(2) 582-590.
[14] M.O. Sonnaillon, G. Bisheimer, C. De Angelo, J. Solsona and G.O. Garc!ıa (2006) "Mechanical-sensor less induction motor drive based only on DC-link measurements" IEE Proc.-Electric. Power Appl., Vol. 153, No. 6